Behavior of GeSbTeBi phase-change optical recording media under subnanosecond pulsed laser irradiation

Kazuo Watabe, Pavel Polynkin, and Masud Mansuripur

We investigated the variations in reflectivity during the phase transition between amorphous and crystalline states of a Bi-doped GeTe–Sb_2Te_3 pseudobinary compound film with subnanosecond laser pulses, using a pump-and-probe technique. We also used a two-laser static tester to estimate the onset time of crystallization under 2.0-μs pulse excitation. Experimental results indicate that the formation of a melt-quenched amorphous mark is completed in ~1 ns, but that crystalline mark formation on an as-deposited amorphous region requires several hundred nanoseconds. Simple arguments based on heat diffusion are used to explain the time scale of amorphization and the threshold for creation of a burned-out hole in the phase-change film. © 2004 Optical Society of America

OCIS codes: 210.0210, 210.4810, 210.4770.

1. Introduction

In rewritable optical data storage, phase-change materials have become mainstream in the marketplace, as they are used for rewritable DVDs such as DVD RAM and DVD RW. In a phase-change medium one, writes and erases data bits by controlling the power of irradiating laser pulses focused onto the recording layer of the medium.[1–5] Writing is carried out by creation of amorphous marks on an initialized, i.e., crystallized, region of the phase-change medium. Such amorphization is induced by melting followed by rapid cooling of the material. A short, relatively high-power pulse focused on the phase-change film causes the film's local temperature to reach beyond the melting temperature T_m of the film, thus causing local melting. Once the pulse has been terminated, the molten pool cools rapidly to form a solid, melt-quenched amorphous mark. The recorded bits are erased by recrystallizing of the amorphous marks. Crystallization is induced by localized annealing. A focused laser beam of moderate power raises the local temperature of the film to its glass-transition point T_g but keeps the temperature below T_m. Maintaining the temperature between T_g and T_m for a sufficient period of time causes the amorphous mark to revert to its crystalline state. Optical readout of the information bits thus recorded requires evaluating the change in reflectivity caused by an array of amorphous marks on a crystalline background. Usually, the amorphous state has lower reflectivity than the crystalline state. A focused cw laser beam at sufficiently low power does not change the local state of the film but reproduces the recorded marks by the change in reflectivity, which is ultimately picked up by a photodetector.

In optical data storage the demand for large capacity and high data transfer rates continues to grow. To achieve a high data rate, one must write data bits (i.e., marks and spaces) in a short time interval, which means that amorphous marks must be formed by short laser pulses. Moreover, direct overwrite of previously recorded marks requires rapid recrystallization as well. Modern optical data storage relies on laser pulses of the order of 10-ns duration, obtained by direct modulation of semiconductor diode lasers. It thus seems natural to investigate pulses of the order of nanosecond or subnanosecond duration to achieve high data transfer rates in future optical storage devices.

The experimental studies of Afonso *et al.*[6] and Siegel *et al.*[7] highlighted reversible amorphization and

K. Watabe (kazuo.watabe@toshiba.co.jp) is with the Core Technology Center, Toshiba Corporation, 8, Shinsugita-cho Isogo-ku, Yokohama 235-8522, Japan. P. Polynkin and M. Mansuripur are with the Optical Sciences Center, University of Arizona, 1630 East University Boulevard, Tucson, Arizona 85721.

Received 24 November 2003; revised manuscript received 24 April 2004; accepted 28 April 2004.

0003-6935/04/204033-08$15.00/0

© 2004 Optical Society of America

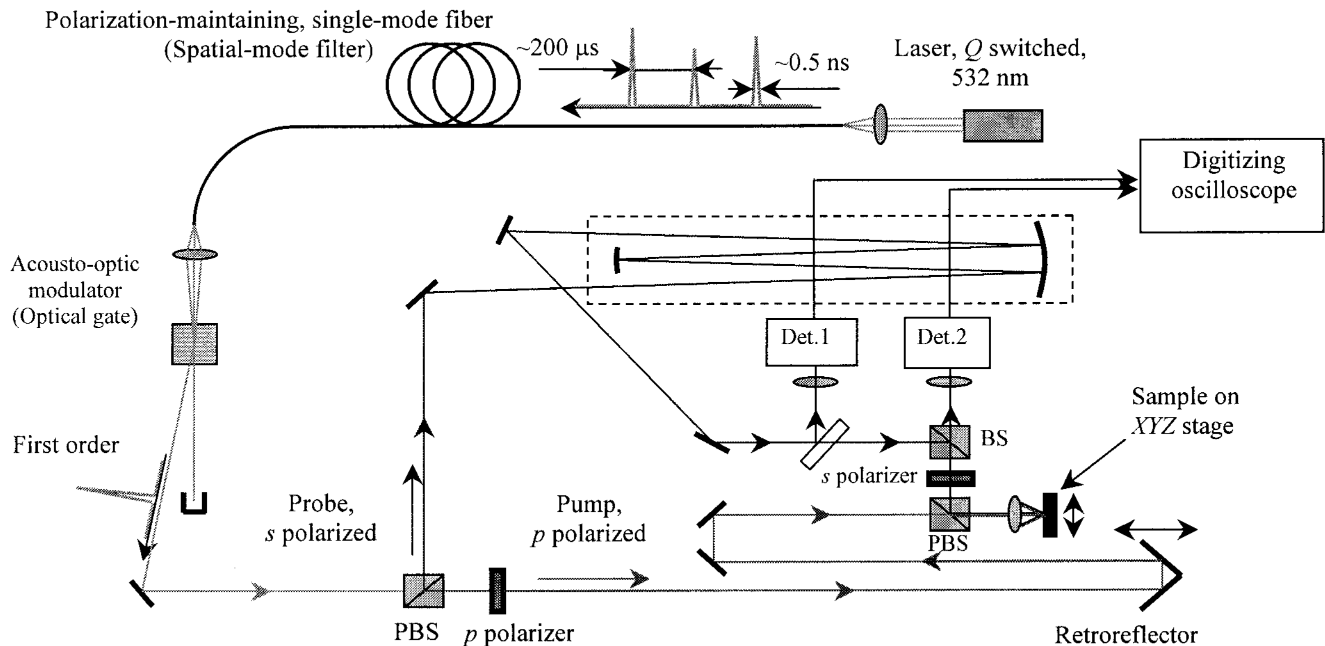

Fig. 1. Schematic of the pump-and-probe tester: Det. 1 and Det. 2, detector 1 and detector 2; PBSs, polarizing beam splitters; BS, beam splitter.

crystallization of phase-change materials under femtosecond and picosecond laser pulses, thus affirming the great potential of this class of material for high-speed rewritable optical data storage applications. At this point, however, there are practical obstacles to implementing femtosecond or picosecond lasers in a practical commercial storage unit. Nevertheless, we remain interested in phase-change phenomena brought about with subnanosecond (i.e., of the order of 0.1 ns) laser pulses, which may be practical for the next generation of rewritable optical data storage products.

In this paper we investigate the transition between amorphous and crystalline phases of a phase-change material induced by a 0.5-ns pulsed laser. A pump-and-probe technique is used to monitor the variation in reflectivity in phase-change events,[8,9] starting just before the onset of the 0.5-ns pulse and continuing throughout and after the end of the pulse. We used quadrilayer samples that contained phase-change films of a GeTe–Sb_2Te_3 pseudobinary composition in which a few percent of Sb was replaced with Bi.[10]

2. Experimental Setup

The experimental setup is shown schematically in Fig. 1. The details of the construction and functioning of the tester are given elsewhere.[8,9] A Q-switched solid-state laser ($\lambda = 532$ nm) is used as the light source. The laser emits a train of pulses whose duration is 0.5 ns and whose repetition rate is 5.7 kHz. We pick a single pulse out of this train with an acousto-optic modulator, which acts as an optical gate. A single pulse is then divided into a pump beam and a probe beam. The probe beam is set to have much weaker intensity, approximately a factor of 40 less than the pump beam, such that it will not affect the phase transition of the sample. We adjust the time delay between the pump and the probe pulses by changing the optical path length of the pump beam, which we do simply by adjusting the position of a retroreflector in its path. The pump and the probe beams are recombined at the second polarizing beam splitter and irradiated onto the sample through a microscope objective. In this research we used a 0.4-N.A. objective lens. The probe coincides at the sample with the pump beam; thus the probe picks up its signal from the central portion of the mark formed by the pump beam, though the reflected signal will be affected by the surroundings of the mark because of the spatial distribution of the focused probe beam at the sample. The signal from the probe is averaged over 20 runs; each run is performed on a fresh point of the sample. (The position of the sample is shifted by 2.5 μm for each run.)

The samples used in this study had a typical quadrilayer structure for front-surface access in which the 0.6-mm-thick substrate is directly beneath the metal (reflective) layer. Figure 2 shows a cross-sectional view of the sample. The stack consists of a 10-nm-thick ZnS–SiO_2 upper dielectric layer, a 13-nm-thick GeSbTeBi phase-change recording layer, a 10-nm-thick (20-nm-thick) ZnS–SiO_2 lower dielectric layer, and a 100-nm-thick silver alloy reflective layer. We hereafter call the sample with the 10-nm-thick lower dielectric layer disk A and the sample with the 20-nm-thick lower dielectric layer disk B. The silver alloy layer acts as a reflector and also as a heat sink, which removes the heat from the phase-change layer deposited there by the laser. Thus we use two kinds of sample that have different thicknesses of the lower dielectric layer and compare their thermal characteristics. We focused the pulsed laser beam through

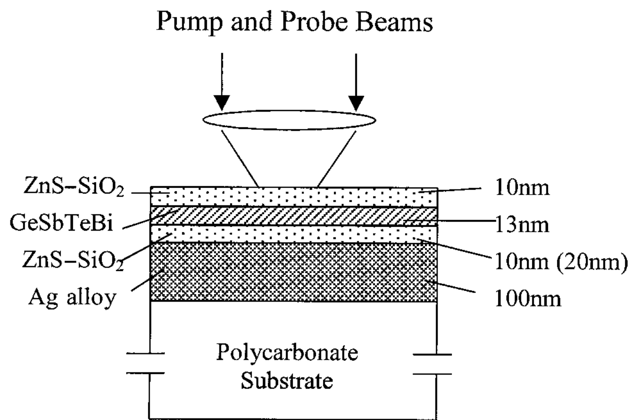

Fig. 2. Structure of the quadrilayer phase-change optical storage medium used in this research.

the upper dielectric layer, and not through the substrate, to eliminate the influence of the birefringence of the substrate, which can cause coherent pump-and-probe cross talk at the signal detector.[9]

The phase-change film in our samples had a GeTe–Sb_2Te_3 pseudobinary composition, with a few percent of Sb replaced by Bi to help the crystallization process by reducing the threshold temperature for crystallization.[10] (This material will be referred to as GSTB film hereafter.) As a result, the recording layer has four elements, namely, Ge, Sb, Te, and Bi. It is believed that crystallization in this type of phase-change film is dominated by growth of nuclei.

We measured the reflectivity for three different states of the phase-change sample, i.e., the as-deposited (amorphous) state, the crystalline state, and the melt-quenched amorphous state. The crystalline state is obtained by annealing of a fairly large as-deposited region of the sample at a moderate temperature. Here, we use a static tester[11,12] to anneal the sample in the as-deposited state by scanning the sample with a focused cw laser beam at a few milliwatts of power. The melt-quenched amorphous state is obtained by irradiation of a previously initialized, i.e., crystallized, area of the sample with a 0.5-ns pulse. We wrote an array of closely spaced melt-quenched amorphous marks upon a crystalline region of the samples by 0.5-ns pulses at 0.25 nJ per pulse. It is conventionally believed that writing amorphous marks so close to one another does not necessarily create a pure melt-quenched amorphous region on phase-change samples. This is so because writing amorphous marks typically creates a crystalline ring about the circular amorphous mark during cooldown where the ring region spends sufficient time in the temperature range between T_g and T_m. In our experiment, however, because of the short duration of the pulse the melt-quenched amorphous marks do not have this crystalline ring about them. We thus create a fairly large melt-quenched amorphous region in our phase-change samples.

The measured reflectivities of the various states for our two samples are listed in Table 1. The reflectivity of the melt-quenched amorphous state was found to be slightly higher than that of the as-deposited state for both disks, in agreement with results reported in the literature.[13,14] Melting and subsequent cooling of a phase-change material can create small crystallites, or crystalline embryos, as the temperature of the film passes through the range between T_g and T_m.[15,16] These embryos raise the reflectivity of the melt-quenched amorphous state slightly above that of the as-deposited state, which presumably does not have any such crystalline embryos.

Table 1. Reflectivities of the Three States of the Phase-Change Samples at λ = 532 nm

Area	Disk A	Disk B
Crystalline area	35.4%	30.8%
As-deposited amorphous area	8.09%	14.51%
Melt-quenched amorphous area	9.26%	14.86%

3. Experiments with Crystalline Film

Localized amorphization of the crystalline state of the storage layer corresponds to writing marks on a phase-change optical disk, which is usually initialized to the crystalline state in advance. Figure 3 shows the measured change in reflectivity during the crystalline-to-amorphous phase change of the GSTB film of disk A. After writing on this sample by short pulses, we bring it to a static tester[11,12] and try to erase (i.e., recrystalize) the marks by using a focused cw laser beam to confirm the state of the marks. Figure 4 shows microscope images of the written marks; the pictures on the right-hand side [Fig. 4(b)] show the marks after erasure. This observation confirms that the bottom curve (corresponding to 0.53 nJ) in Fig. 3 represents the formation of a permanent hole in the film rather than a melt-quenched amor-

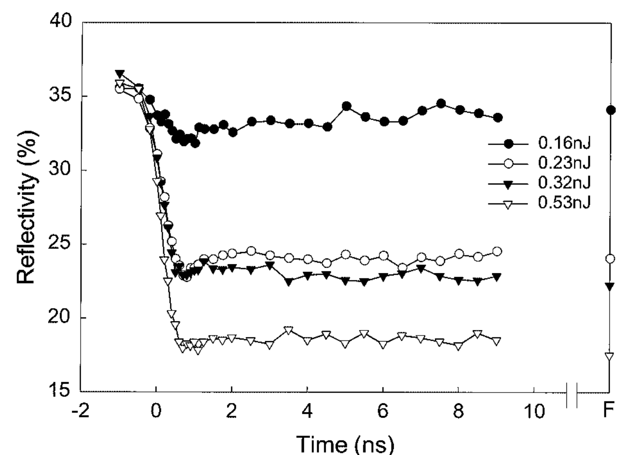

Fig. 3. Variations in reflectivity during amorphization of the crystalline state of Bi-doped pseudobinary GeSbTe film (disk A). Each curve corresponds to a specific value of the pulse energy. All the pulses have durations of 0.5 ns. The rightmost point of each curve represents the final reflectivity of the recorded mark (after several minutes).

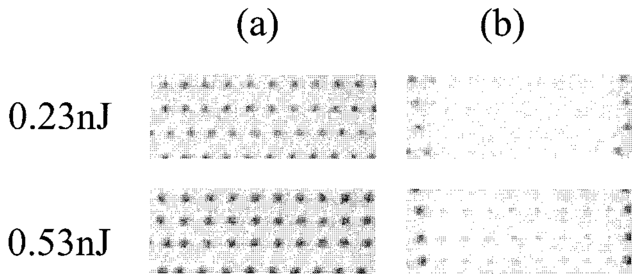

Fig. 4. (a) Optical microscope images of amorphous marks written on a crystalline GSTB film (disk A). (b) The marks in the central region of the imaged frames were erased by a focused cw laser beam (mark spacing, 2.5 μm in the horizontal direction).

phous mark (Fig. 4, bottom). Marks written at 0.16 nJ are hardly discernible from the crystalline background under an optical microscope, even though at least a tiny mark is expected to have formed as expected from the information in Fig. 3 by the slight drop in the reflectivity of the sample. The two curves in the middle of Fig. 3 illustrate the formation of distinguishable melt-quenched amorphous marks. In these cases, the reflectivity drops immediately after the beginning of the pulse ($t = 0.0$ ns) and reaches its lowest value at the end of the pulse ($t = 0.5$ ns). After reaching minimum, the reflectivity goes up ever so slightly for several hundred picoseconds before reaching its final value; this corresponds to the cooling–solidification process. If we suppose that thermal conductivity K and specific heat C of the GSTB film and dielectric layers are nearly the same as inferred from other sources ($K = 0.005$ J/cm/s/°C, $C = 1.5$ J/cm^3/°C),[15] we can estimate how far the heat flows during laser exposure. In a time t, heat diffuses a typical distance $L = (Kt/C)^{1/2}$, which, for $t = 0.5$ ns, yields a value for L of ~13 nm.[17] Thus immediately after the 0.5-ns duration of the pulse the heat can reach the heat-sinking layer (i.e., the Ag alloy), which, because of its high thermal conductivity, diffuses heat rapidly. Consequently, one can safely say that the melt-quenched amorphous mark forms in ~1 ns.

Besides the melt-quenched amorphous marks, it is interesting to note that a permanent hole is also formed in the time interval of 1 ns. We expect this hole to be within the recording layer and not a through hole (i.e., all the way to the plastic substrate), as there is not enough energy in the pulse to melt the fairly thick metal layer.

4. Experiments with As-Deposited Amorphous Film

A. Disk A: 10-nm Lower Dielectric Layer

Figure 5 shows reflectivity traces obtained during laser irradiation of the as-deposited GSTB film of disk A. The energy content of the pulse is varied from 0.05 to 0.40 nJ. We can crystallize the as-deposited region by maintaining its temperature long enough between glass transition temperature T_g and melting temperature T_m.[16,17] Investigation of the final reflectivities in Fig. 5 reveals that none of the curves corresponds to crystalline mark formation, and inspection under the static tester shows that writing with 0.20-nJ or higher-energy pulses produces unerasable marks (i.e., hole opening). Figure 6 shows optical microscope images of the written marks. These amorphous marks can be seen to have slightly higher reflectivity than the as-deposited amorphous background. It is clear that marks written with 0.31 nJ of energy contain a dark burned-out hole at the center. With careful inspection, one can even see the small burned-out holes formed during writing by 0.20-nJ pulses.

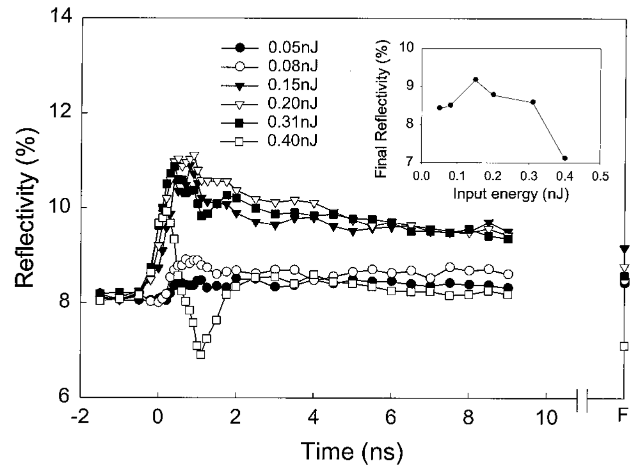

Fig. 5. Variations in reflectivity during short-pulse laser irradiation of the as-deposited GSTB film (disk A). Each curve corresponds to a specific value of pulse energy. All pulses have duration $\tau = 0.5$ ns. The rightmost data point for each curve represents the final reflectivity after several minutes. The dependence of this final reflectivity on pulse energy is shown in the inset. The background reflectivity of 8.09% represents the value at zero input energy.

The inset of Fig. 5 shows a plot of final reflectivity versus pulse energy. Here, reflectivity is a maximum at 0.15 nJ and drops after this point with the increasing pulse energy (owing to the formation of

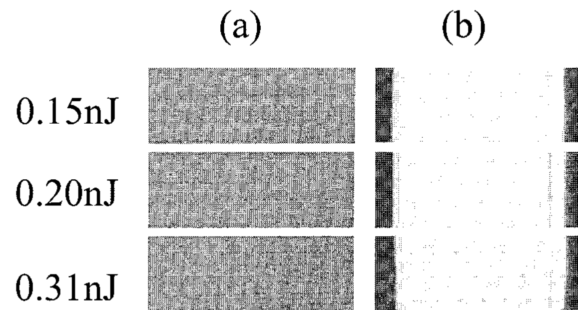

Fig. 6. (a) Optical microscope images of amorphous marks written on the as-deposited amorphous GSTB film (disk A). The marks in the central region of imaged frames were erased by a focused cw laser beam. The vertical dark lines in the images of (b) represent holes burned out not during short-pulse writing but during erasure by raster scanning (mark spacing, 2.5 μm in the horizontal direction).

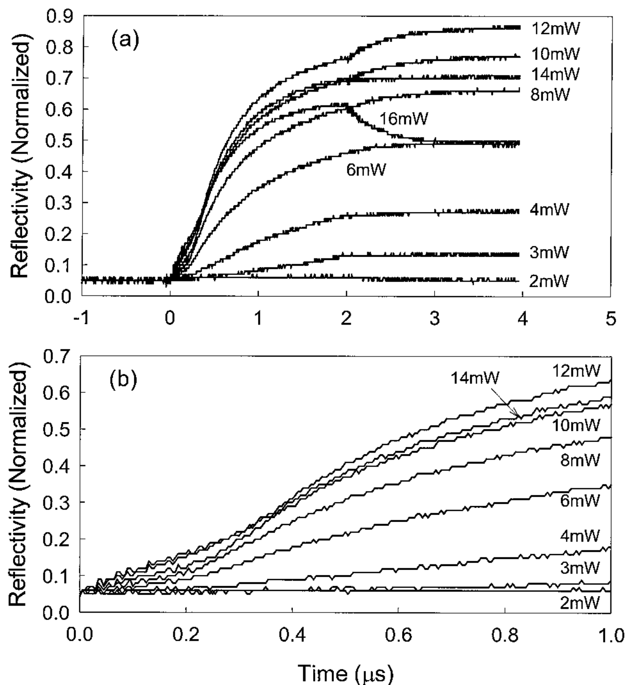

Fig. 7. Variations in reflectivity during long-pulse laser irradiation of the as-deposited GSTB film (disk A). Each curve corresponds to a specific value of the pulse power. All pulses have 2.0-μs duration. Reflectivity is normalized by its value for the crystalline state of the sample. Each curve is averaged over 20 identical trials at different locations on the sample. A close-up of variations in reflectivity is shown in (b).

burned-out holes). The peak reflectivity is comparable to the value measured for the melt-quenched amorphous state of the sample; see Table 1. We could not record polycrystalline marks on this sample even though we decreased the energy of the short pulse to very low values, e.g., 0.05 nJ, to prevent melting. This result, of course, is expected because the GSTB film does not have enough time to generate nucleation sites throughout the illuminated region with these short pulses.

Next, we conducted experiments on the static tester with relatively long pulses on the as-deposited amorphous region of disk A to estimate the approximate onset time of crystallization for this medium. Figure 7 shows variations in reflectivity during the formation of crystalline marks on the as-deposited region of disk A on application of a 2.0-μs pulse (pulse duration, 0–2.0 μs in the figure). The reflectivity is normalized by its value for the crystalline state of the sample. The experiments are conducted on a static tester,[11,12] which has two semiconductor lasers operating at $\lambda_1 = 680$ nm (laser 1) and $\lambda_2 = 643$ nm (laser 2). We used laser 1 as a pump beam for writing and laser 2 as a probe beam for reading. A 0.6-N.A. microscope objective was used to focus both beams onto the same spot at the sample.

This type of transition from the as-deposited amorphous state to the crystalline state has been well investigated in the literature.[15,18] In Fig. 7 the reflectivity for all the curves starts from its value for the as-deposited state and reaches its final value near 3–4 μs. Subsequent erasure experiments show that marks written at 16 mW have burned-out holes at the center. We see no indication of mark formation on irradiation with 2.0-mW pulses. Otherwise crystalline marks were formed with pulses from 4.0 to 14.0 mW, and they were found to be erasable. The difference in the final reflectivity observed for different write powers is caused by differences in the final sizes of the recorded marks. The highest reflectivity, and consequently the largest mark, was obtained at 12.0-mW write power.

To permit these transition processes to be inspected in detail, we provide in Fig. 7(b) a close-up view of some of the curves in Fig. 7(a). In the time range between 0 and 0.2 μs we find that the reflectivity takes off immediately after $t = 0$, especially for pulse powers greater than 4 mW. This is likely caused by the change in the optical constants of the sample with rising temperature.[15,18] Taking this effect into account, we can estimate the onset time of crystallization as ~200 ns, except for the lower two curves (3 and 2 mW); one of them shows a longer onset time, and the other may have no crystallization onset at all. The curve that corresponds to 14.0 mW of pulse power shows a lower crystallization rate than that of the 12.0-mW curve, presumably because at higher power the temperature at the center of the beam spot exceeds the melting point, which creates a small amorphous region at the center of the spot that depresses the reflectivity.

From Fig. 5, the pulse duration of 0.5 ns turns out to be too short for this film to enable crystallization of the as-deposited amorphous state to take place. It is thus possible, with 0.5-ns laser pulses, to form melt-quenched amorphous marks without forming crystalline rings around them. Thus the melt-quenched area formed by an array of closely spaced melt-quenched marks discussed in Section 2 (in conjunction with Table 1) should be a pure melt-quenched amorphous state without any recrystallized areas.

The results of the crystalline-to-amorphous and amorphous-to-crystalline transitions discussed so far lead to the following conclusion: Even though a phase-change medium may exhibit an amorphous-to-crystalline transition in hundred-nanosecond or longer time frames, it can nevertheless form melt-quenched amorphous marks in 1 ns or less, induced by a subnanosecond laser pulse.

B. Disk B: 20-nm Lower Dielectric Layer

Figure 8 shows measured variations in reflectivity that resulted from a 0.5-ns pulse irradiation on the as-deposited region of the GSTB film of disk B. Experimental conditions for this measurement were the same as those used in our previous experiments with disk A (Fig. 5). The energy per pulse varied from 0.08 to 0.33 nJ.

The minimum reflectivity was attained near 0.6 or 0.7 ns for all the curves except that with an energy of 0.33 nJ. This result suggests the formation of a different structure by the 0.33-nJ pulse, as we discuss

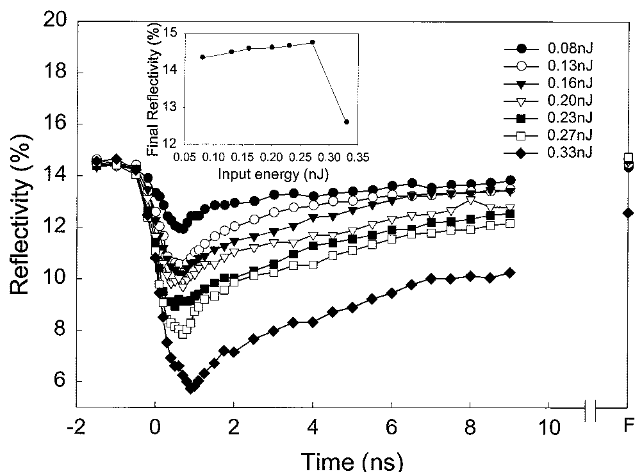

Fig. 8. Variations in reflectivity during short-pulse laser irradiation of the as-deposited GSTB film (disk B). Each curve corresponds to a specific value of the pulse energy. All pulses have 0.5-ns duration. The rightmost point of each curve represents the final reflectivity of the corresponding mark after several minutes. The dependence of this final reflectivity on pulse energy during short-pulse irradiation is shown in the inset. The background reflectivity of 14.51% represents the value at zero input energy.

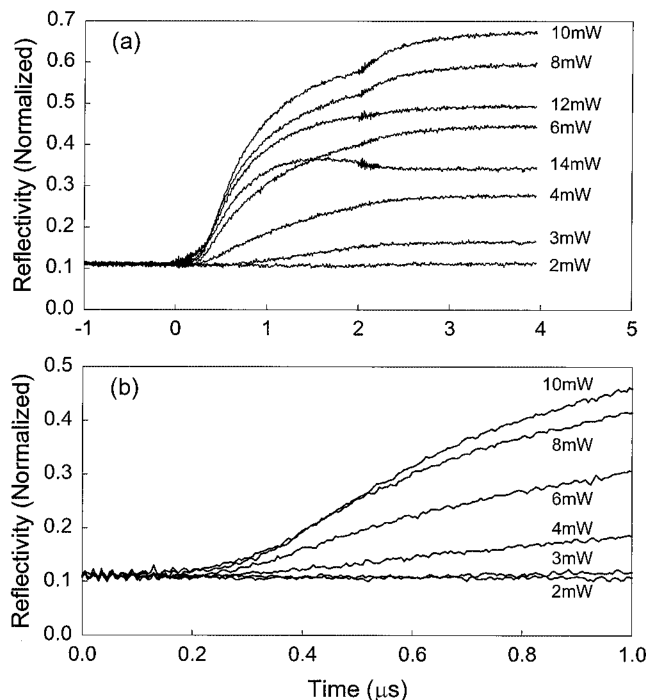

Fig. 9. Variations in reflectivity during long-pulse irradiation of the as-deposited GSTB film (disk B). Each curve corresponds to a specific value of the pulse power. All pulses have 2.0-μs duration. Reflectivity is normalized by its value for the crystalline state of the sample. Each plot is averaged over 20 identical trials at different locations on the sample. A close-up of variations in reflectivity is shown in (b).

below. Considering the final reflectivities, whose values are comparable to the initial value for the as-deposited amorphous film, the final state of the mark in none of these experiments must be crystalline, similar to the results obtained for disk A. The marks written with 0.20 nJ of energy or more were found to contain permanent burned-out regions after erasure on the static tester. This energy threshold is nearly the same as that for disk A, despite the disks' having different lower dielectric layer thicknesses, though the thicker dielectric layer should give disk B a relatively slow cooling rate and a correspondingly low threshold energy for burn-out. Using heat diffusion arguments, we can understand this phenomenon as follows: Within 0.5 ns the heat applied to the GSTB film does not have enough time to diffuse to the heat-sinking layer because the combined thickness of the lower dielectric layer and the GSTB film is greater than the diffusion length on this time scale. Thus all the energy input to the medium is absorbed in the GSTB film during the pulse, irrespective of the thickness of the lower dielectric layer. Therefore, simply determined by the input energy, the threshold of permanent burn-out is the same for disks A and B.

The inset of Fig. 8 shows the final reflectivities obtained a few minutes after pulse irradiation. The final reflectivity increases ever so slightly as the energy per pulse increases at first. This increase is caused by the formation of melt-quenched amorphous marks that have slightly higher reflectivity than the as-deposited film; see Table 1. We inspected the written marks under an optical microscope and observed that the marks written with 0.20–0.27 nJ of energy have burned-out holes surrounded by melt-quenched amorphous rings. Therefore at 0.20 nJ the increase in reflectivity appears to slow down with the creation of dark, burned-out holes. However, the increase in the area of the melt-quenched amorphous ring surrounding the hole keeps the reflectivity on a rising path. The final reflectivity obtained with a 0.33-nJ pulse shows by far the lowest value in Fig. 8. For the marks written with 0.33 nJ, we found a structure different from those written at lower energy. Those marks have a dark annular region surrounding a bright spot in the center, probably as a result of a permanent structural change in the reflective metal layer as well as in the GSTB layer, whereas the previously noted burned-outs at lower energies are structural changes in the GSTB film alone.

Next, writing experiments with disk B were performed on a static tester with a 2.0-μs rectangular pulse similar to that used for disk A. Figure 9 shows variations in reflectivity on irradiation of the as-deposited area of disk B. With 12.0 and 14.0 mW, marks were found to have burned-out holes, whereas marks formed with lower powers could be fully erased on the static tester. The curves in Fig. 9 share characteristics similar to those of Fig. 7, which was obtained for disk A. Focusing on the differences between the results with disks A and B, we found the threshold power for burn-out to be lower for disk B, unlike in the short-pulse experiment. This result is not surprising, considering that heat diffusion now occurs over time intervals much shorter than the pulse duration of 2.0 μs. The different thicknesses

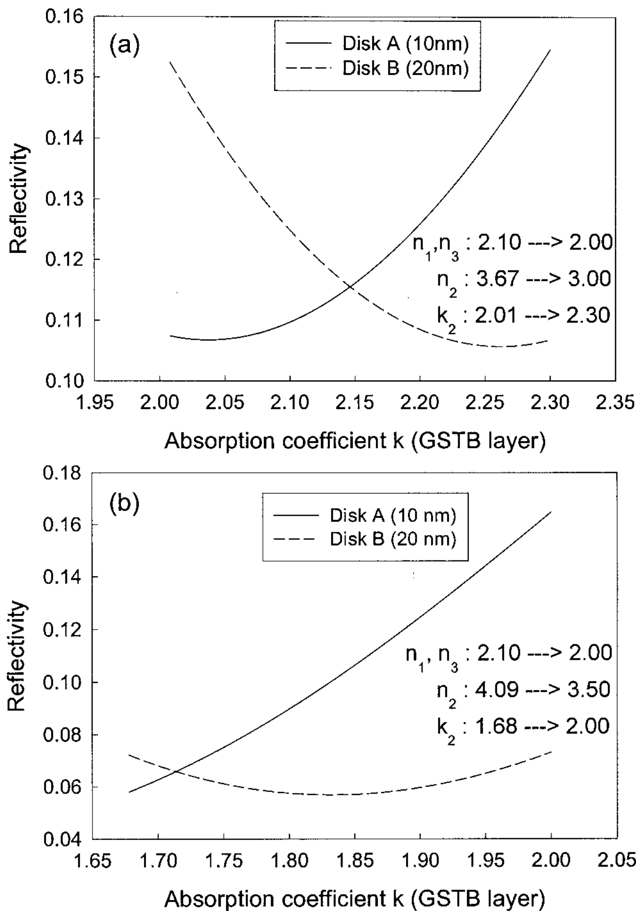

Fig. 10. Calculated variations in reflectivity of disks A and B during heating [(a) $\lambda = 532$ nm, (b) $\lambda = 643$ nm]. The temperature dependences of the optical constants of each layer are listed in Table 2. All the parameters are changed simultaneously, though only the absorption coefficient k of the GSTB layer is shown in the horizontal axis.

of the lower dielectric layer thus matter under long-pulse irradiation. Disk A, which has a thin upper layer, cools faster during the pulse, thus pushing the threshold power higher than that for disk B.

Finally, the close-up view of the reflectivity curves of Fig. 9(a) that is shown in Fig. 9(b) indicates that for disk B reflectivities do not rise significantly until ~200 ns. Apparently, the change in the optical constants of this sample with rising temperature does not cause much change in the reflectivity of the stack. It is thus easier to determine the onset time of crystallization for the GSTB film of disk B than it was for disk A. These times should coincide, as the two disks have identical GSTB films and, not surprisingly, we found the same value for the onset time of crystallization, namely, ~200 ns.

C. Discussion of the Change in Reflectivity with Rising Temperature

Comparing the results of Figs. 5 (for disk A) and 8 (for disk B), we noticed a basic difference in the curves.

Table 2. Optical Constants of the Quadric-Layer Stacks at Room Temperature and at an Elevated Temperature

Layer	Refractive Index (n)	Absorption Coefficient (k)	n (heated)	k (heated)
$\lambda = 532$ nm				
ZnS–SiO_2	2.099	0.052	2.000	0.052
GeSbTeBi	3.672	2.008	3.000	2.300
Ag alloy	0.120	3.330	—	—
$\lambda = 643$ nm				
ZnS–SiO_2	2.099	0.040	2.000	0.040
GeSbTeBi	4.092	1.678	3.500	2.000
Ag alloy	0.128	4.281	—	—

Unlike the results for disk A, every curve in Fig. 8 decreases in reflectivity on irradiation by the pulse. This may be due to the change in optical constants with temperature combined with the effect of coherent optical interference among various layers of each disk. Figure 10 shows the calculated variations in reflectivity of the two disks during heating. The results for the wavelength of 532 nm are shown in Fig. 10(a). The optical constants used for both disks are listed in Table 2. The refractive indices of the dielectric layer and the phase-change recording layer are believed to decrease with rising temperature, whereas the absorption coefficient of the phase-change film is expected to increase with rising temperature. Thus we changed the constants, as given in Table 2, for calculating the reflectivity variations of our media. We did not change the indices of the metal reflective layer because that layer should not be heated much compared with to the other layers. In Fig. 10, all parameters were changed simultaneously, although the x axis of the figure shows only absorption coefficient k of the GSTB layer. The change in the optical constants of disk A favors an increase in reflectivity, whereas for disk B it results in a decrease in reflectivity, in good agreement with the experimental results shown in Figs. 5 and 8. Even though the two disks differ (by 10 nm) only in the thickness of the lower dielectric layer, this difference appears to be sufficient to cause the observed changes in reflectivity on multiple reflections within the multilayer stack.[17]

Figure 10(b) shows the calculated reflectivity variation for $\lambda = 643$ nm to simulate the results obtained with the static tester. The optical constants for this calculation are also given in Table 2. The changing the optical constants of disk A caused an increase in reflectivity with rising temperature, whereas for disk B they resulted in only a slight change. This result again agrees well with the experimental results shown above in Figs. 7 and 9.

5. Conclusions

Variations in reflectivity during phase transition between the amorphous and crystalline states of two quadrilayer phase-change samples have been investigated with subnanosecond laser pulses by use of a pump-and-probe technique. We created a melt-quenched amorphous mark on the precrystallized

area of a Bi-doped GeTe–Sb_2Te_3 pseudobinary phase-change sample with a 0.5-ns laser pulse. This crystalline-to-amorphous transition was found to complete its course within ~1 ns. Crystalline formation on the as-deposited amorphous state of this medium did not start on application of a 0.5-ns pulse but required at least 200 ns under 2.0-μs laser pulse irradiation. Simple arguments based on heat diffusion were used to explain qualitatively the time scale of amorphization and the threshold energy for creation of burned-out holes within the phase-change film.

The authors are grateful to H. Satoh, H. Ohsawa, N. Nakamura, N. Oomachi, and S. Ashida of the Toshiba Corporation of Japan for providing the phase-change samples for this study.

References

1. J. Feinleib, J. deNeufville, S. C. Moss, and S. R. Ovshinsky, “Rapid reversible light-induced crystallization of amorphous semiconductors,” Appl. Phys. Lett. **18,** 254–257 (1971).
2. R. J. von Gutfeld and P. Chaudhari, “Laser writing and erasing on chalcogenide films,” J. Appl. Phys. **43,** 4688–4693 (1972).
3. D. J. Gravesteijn, “Materials developments for write-once and erasable phase-change optical recording,” Appl. Opt. **27,** 736–738 (1988).
4. H. Minemura, H. Andoh, N. Tsuboi, Y. Maeda, and Y. Sato, “Three-dimensional analysis of overwritable phase-change optical disks,” J. Appl. Phys. **67,** 2731–2735 (1990).
5. Y. Maeda, I. Ikuta, H. Andoh, and Y. Sato, “Single-beam overwrite with a new erase mode of In_3SbTe_2 phase-change optical disks,” Jpn. J. Appl. Phys. **31,** 451–455 (1992).
6. C. N. Afonso, J. Solis, F. Catalina, and C. Kalpouzos, “Ultrafast reversible phase change in GeSb films for erasable optical storage,” Appl. Phys. Lett. **60,** 3123–3125 (1992).
7. J. Siegel, C. N. Afonso, and J. Solis, “Dynamics of ultrafast reversible phase transitions in GeSb films triggered by picosecond laser pulses,” Appl. Phys. Lett. **75,** 3102–3104 (1999).
8. C. Peng, J. K. Erwin, and M. Mansuripur, “Amorphization induced by subnanosecond laser pulses in phase-change optical recording media,” Appl. Opt. (to be published).
9. K. Watabe, P. Polynkin, and M. Mansuripur, “Optical pump-and-probe test system for thermal characterization of thin metal and phase-change films,” Appl. Opt. (to be published).
10. K. Yusu, S. Ashida, N. Nakamura, N. Oomachi, N. Morishita, A. Ogawa, and K. Ichihara, “Advanced phase change media for blue laser recording of 18 GB capacity for 0.65 numerical aperture and 30 GB capacity for 0.85 numerical aperture,” Jpn. J. Appl. Phys. **42,** 858–862 (2003).
11. M. Mansuripur, J. K. Erwin, W. Bletscher, P. K. Khulbe, K. Sadeghi, X. Xun, A. Gupta, and S. B. Mendes, “Static tester for characterization of phase-change, dye-polymer, and magneto-optical media for optical data storage,” Appl. Opt. **38,** 7095–7104 (1999).
12. M. Mansuripur, P. K. Khulbe, X. Xun, J. K. Erwin, and W. Bletscher, “Real-time studies of mark formation processes in phase-change and magneto-optical media using a two-laser tester,” J. Magn. Soc. Jpn. **25,** 399–407 (2001).
13. J. H. Coombs, A. P. J. M. Jongenelis, W. van Es-Spiekman, and B. A. J. Jacobs, “Laser-induced crystallization phenomena in GeTe-based alloys. I. Characterization of nucleation and growth,” J. Appl. Phys. **78,** 4906–4913 (1995).
14. P. K. Khube, T. Hurst, M. Horie, and M. Mansuripur, “Crystallization behavior of Ge-doped eutectic $Sb_{70}Te_{30}$ films in optical disks,” Appl. Opt. **41,** 6220–6229 (2002).
15. P. K. Khulbe, E. M. Wright, and M. Mansuripur, “Crystallization behavior of as-deposited, melt quenched, and primed amorphous states of $Ge_2Sb_{2.3}Te_5$ films,” J. Appl. Phys. **88,** 3926–3933 (2000).
16. E. M. Wright, P. K. Khulbe, and M. Mansuripur, “Dynamic theory of crystallization in $Ge_2Sb_{2.3}Te_5$ phase-change optical recording media,” Appl. Opt. **39,** 6695–6701 (2000).
17. A. B. Marchant, *Optical Recording* (Addison-Wesley, Reading, Mass., 1990).
18. P. K. Khulbe, X. Xun, and M. Mansuripur, “Crystallization and amorphization studies of a $Ge_2Sb_{2.3}Te_5$ thin-film sample under pulsed laser irradiation,” Appl. Opt. **39,** 2359–2366 (2000).